Relative distance measurements using inter-satellite optical communication links

Jain, R.; Speretta, S.; Dirkx, D.; Gill, E.K.A.

DOI
10.1117/12.3001467

Publication date
2024

Document Version
Final published version

Published in
Free-Space Laser Communications XXXVI

Relative distance measurements using inter-satellite optical communication links

Rashika Jain[a], Stefano Speretta[a], Dominic Dirk[a], and Eberhard Gill[a]

[a]Delft University of Technology, Kluyverweg 1, Delft, 2629 HS, The Netherlands

ABSTRACT

The need for higher data rates has transitioned the satellites towards laser communication, opening up new opportunities for inter-satellite distance measurements. The stringent requirements for space missions like gravimetry, formation flying, collision avoidance, and precise orbit determination require highly precise distance knowledge, which can be offered by lasers. The past and present missions depend on radio ranging and laser interferometers to achieve up to centimeter-order and picometer-order precision, respectively. However, these methods either require additional hardware or interfere with the communication data rates as the power available is shared between communication and ranging operations. Therefore, this research explores the potential of laser communication terminals in measuring the inter-satellite distance. Numerical simulations are performed to analyze the effect of the precision of inter-satellite distance measurements on atmospheric density estimation. The analysis shows that such range measurements can only improve atmospheric density estimates if the uncertainty in the drag coefficient can be reduced below the current range of 3-5%.

Keywords: inter-satellite distance, laser communication, data-aided ranging, inter-satellite ranging, formation flying

1. INTRODUCTION

Small satellites work together in formations as they have distinct advantages over large spacecraft, such as the ability to measure from multiple angles and perspectives. To maintain and control the formation, a precise knowledge of the distance between the satellites is required.[1] This distance can be measured using inter-satellite ranging, which is accomplished through direct or indirect methods.[2] A range measurement is typically the time-of-flight or phase shift of a radio or optical signal, which is then converted to distance.[3]

Direct methods can provide more accurate measurements as the ranging signal is not subject to atmospheric interference, and satellites do not have to wait for a ground station pass to perform ranging. For example, using microwave ranging data along with the Global Navigation Satellite System (GNSS) data, the relative accuracy of GRACE-FO Precise Orbit Determination (POD) orbits increased from 5.7 mm to 0.2 mm.[4]

In the radio domain, direct range measurements can be multiplexed with communication, as both signals can be added and then phase modulated. However, it limits the power available for communication and reduces the achievable data rate, a crucial requirement for most missions. In contrast, such multiplexing is not yet possible in the optical domain as the optical signals are modulated using On-Off Keying (OOK) or Pulse Position Modulation (PPM).[5] As a result, a separate ranging system is required on each satellite, which can increase the mission's complexity, costs, and SMaP (size, mass, and power) requirements. Hence, research is ongoing to perform ranging from satellite communication signals, which removes the need for separate ranging systems in the optical domain[6,7] and reduces the power consumption for radio systems.[8–13]

Further author information: (send correspondence to R. Jain)
R. Jain: Space Systems Engineering Section, Faculty of Aerospace Engineering, Kluyverweg 1; r.jain-1@tudelft.nl
S. Speretta: Space Systems Engineering Section, Faculty of Aerospace Engineering, Kluyverweg 1; s.speretta@tudelft.nl
D. Dirkx: Astrodynamics and Space Missions Section, Faculty of Aerospace Engineering, Kluyverweg 1; d.dirkx@tudelft.nl
E.K.A. Gill: Space Systems Engineering Section, Faculty of Aerospace Engineering, Kluyverweg 1; e.k.a.gill@tudelft.nl

Free-Space Laser Communications XXXVI, edited by Hamid Hemmati, Bryan S. Robinson, Proc. of SPIE Vol. 12877, 128771O
 · 0277-786X · doi: 10.1117/12.3001467

This research focuses on developing a laser communication terminal with inter-satellite ranging capabilities that interfere as little as possible with the system's data transmission capabilities. This paper presents the potential application of precise inter-satellite distance measurements taken using such a system to estimate atmospheric density from a two-satellite Along-track Orbit (ATO) formation. In Sections 2 and 3, the methodology and the setup of the numerical simulations are explained, respectively. Section 4 gives the results of the simulations with a detailed discussion. The paper concludes with an overview of future work in Section 5.

2. METHODOLOGY

Satellites in the Low-Earth Orbit (LEO) experience drag due to the presence of the atmosphere. The acceleration due to drag (a_{drag}) acting on the satellite is related to the local atmospheric density (ρ) by Eq. (1),

$$a_{drag} = \frac{1}{2}\rho v^2 C_D \frac{A}{m}\,, \tag{1}$$

where v is the speed of the satellite relative to the atmosphere, C_D is the drag coefficient, and A/m is the area-to-mass ratio of the satellite. Therefore, the drag data from satellites in LEO is used to estimate thermospheric density and improve existing atmospheric models, such as the NRLMSISE model, which can compute density with 15% uncertainty.[14] A better estimation of atmospheric density is needed to improve the orbit prediction of future satellites.

In this paper, different types of data available onboard the satellite are modeled and used to estimate the density. A scale factor (f) is introduced, such that the true density (ρ) is a piecewise constant of the nominal density ($\widetilde{\rho}$) obtained from the NRLMSISE model. The relation can be written as:

$$\rho \approx f \times \widetilde{\rho}\,, \tag{2}$$

and holds under the assumption that uncertainties in all other parameters in Eq. (1) are negligible compared to the uncertainty in thermospheric density.[15] f is a force model parameter and can be estimated with the satellites' initial states in the POD process.[3] Substituting Eq. (2) in Eq. (1) gives Eq. (3), which will be the base of numerical simulations.

$$a_{drag} = \frac{v^2 A}{2m}(f\widetilde{\rho})\; C_D\,. \tag{3}$$

For the simulations, an ATO formation in LEO of two 3U-CubeSats (i.e., one satellite follows the other on the same orbit with some initial separation) with different A is used, assuming both satellites have onboard optical communication and ranging systems to establish an Inter-Satellite Link (ISL). The different cross-sectional areas will result in differential drag, leading to variations in the inter-satellite distance throughout the orbit. These distance measurements will help to determine the drag coefficient of both satellites and thus will be added as observables to POD. To make the estimation model compatible with the numerical simulation tool, Eq. (3) is rewritten as Eq. (4), and it is assumed that the uncertainty in density is instead an uncertainty in C_D, and the knowledge of density from the model is exact. Therefore, the problem has now changed from density estimation to estimation of C_D ($= f \times \widetilde{C}_D$), where $\widetilde{C}_D$ is the nominal drag coefficient.

$$a_{drag} = \frac{v^2 A}{2m}\widetilde{\rho}\;(f\widetilde{C}_D)\,. \tag{4}$$

Using covariance analysis,[3,16] the design matrix H is formed from a set of modeled observations (h) and a set of parameters to be estimated (q), as given in Eq. (5). The set q includes the position ($\boldsymbol{r}$), velocity ($\boldsymbol{v}$), and arc-wise C_D of both satellites. To account for the variations in the atmospheric density, C_D is estimated over shorter arcs. The set h includes the modeled direct inter-satellite range (r_{12}) to study the effect of ISL on density estimation. Further, to make the system observable and well-posed, modeled GNSS positions of both the satellites ($\boldsymbol{r}_{G1}$, $\boldsymbol{r}_{G2}$) are also added to h.

$$H = \frac{\partial h}{\partial q},\ h = \begin{pmatrix} r_{12} \\ \boldsymbol{r}_{G1} \\ \boldsymbol{r}_{G2} \end{pmatrix},\ q = \begin{pmatrix} \boldsymbol{r_1}(t > t_0) \\ \boldsymbol{v_1}(t > t_0) \\ \boldsymbol{r_2}(t > t_0) \\ \boldsymbol{v_2}(t > t_0) \\ C_{D_1} \\ C_{D_2} \end{pmatrix}. \tag{5}$$

The design matrix calculated in Eq. (5) contains the contribution of C_D of both satellites separately. Therefore, to consider their collective effect, the matrix H is modified such that:

$$\frac{\partial h}{\partial C_D} = \frac{\partial h}{\partial C_{D_1}} + \frac{\partial h}{\partial C_{D_2}}. \tag{6}$$

The covariance matrix, P, is computed from Eq. (7), where W is the weight matrix of the observations, and P_0 is the a priori covariance matrix. W is set as a diagonal matrix with $W_{ii} = \sigma_{h,i}^{-2}$, where $\sigma_{h,i}$ denotes the uncertainty of observation i assuming Gaussian, zero-mean, time-uncorrelated, noise.

$$P = (H^T W H + P_0^{-1})^{-1}. \tag{7}$$

The uncertainty in the GNSS positions is obtained from past missions, and the inter-satellite ranging accuracy will be derived from the characteristics of the optical communication terminal. All the random errors are added as zero-mean Gaussian noise to the modeled observations.

The standard deviation of the estimated parameters can then be computed from the covariance matrix as $\sigma_{q,i} = \sqrt{P_{ii}}$. Therefore, the relative uncertainty in the scaling factor f can be computed from the achieved uncertainty in C_D and the estimated C_D using Eqs. (8) and (9).

$$f = \frac{f\widetilde{C}_D}{\widetilde{C}_D} = \frac{C_D}{\widetilde{C}_D}, \tag{8}$$

$$\left(\frac{\sigma_f}{f}\right)^2 = \left(\frac{\sigma_{C_D}}{C_D}\right)^2 + \left(\frac{\sigma_{\widetilde{C}_D}}{\widetilde{C}_D}\right)^2. \tag{9}$$

The first part of the right-hand side of Eq. (9) is the result of the simulations, and the second part is our knowledge of the drag coefficient. The value of $\frac{\sigma_f}{f}$ signifies the improvement that can be achieved in the density estimates using the inter-satellite optical link. The following section describes the setup of the simulations.

3. SIMULATIONS

Numerical simulations were carried out using the orbital parameters of the leader satellite given in Table 1. The follower satellite is at an initial relative distance of 12 km, i.e., $\Delta\nu = 0.1°$, and is rotated by 90°, such that the leader has three times the reference area of the follower. Thus, the leader satellite will experience more drag, leading to variations in the inter-satellite distance throughout the orbit. Although the computation of C_D is not trivial and depends on various factors, a nominal value of 2.2 is usually used along with a 5% uncertainty in the a priori knowledge[15] (second part of Eq. (9)). Besides, an uncertainty of 15 m is assumed in the GNSS positions of both satellites.

Table 1: Orbital parameters of the leader satellite.

Perigee (r_p)	400 km
Eccentricity (e)	0.01
Inclination (i)	87.18°
Argument of Perigee (ω)	277.62°
RAAN (Ω)	124.21°
True anomaly (ν)	139.87°

4. RESULTS

The random noise in the inter-satellite range measurements is varied from cm to km, and its effect is analyzed on the accuracy of the estimation of atmospheric density. The uncertainty in the drag coefficient is then computed by performing a covariance analysis as described in the methodology with an arc length of 30 minutes for half a day, i.e., eight orbits.

Fig. 1 depicts the variation of the uncertainties in the arc-wise drag coefficient over time for four distinct noise levels in inter-satellite range measurements. The dashed line indicates the outcome of the simulations when only GNSS positions are used as observations, and no direct ISL is added. Two trends can be seen; firstly, adding direct range measurements between the two satellites reduces the uncertainty in C_D, which is expected because direct measurements carry more information about the local orbital dynamics than GNSS measurements. Secondly, the uncertainty in C_D increases with the increase in the ISL ranging noise, which is as expected because increasing the noise decreases the weight of the modeled observations in W in Eq. (7). As a result, at greater noise levels, the uncertainty in C_D approaches the GNSS-only values.

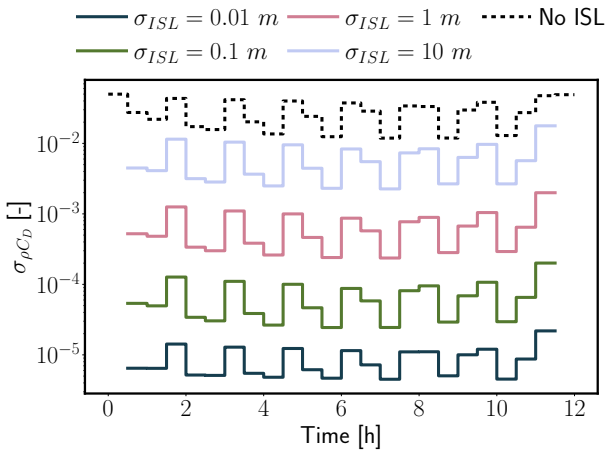

Figure 1: Plot of the arc-wise standard deviation of the drag coefficient σ_{C_D} as a function of time for four levels of Inter-Satellite Ranging noise σ_{ISL} with an integration time of 1 s. The dotted line represents the observation model with only GNSS positions and without ISL range measurements.

Further, to investigate the uncertainty in the scaling factor introduced in the methodology, the uncertainty in the arc-wise drag coefficient is averaged over all arcs as shown in Fig. 2a. The curves begin to flatten once the noise in the ISL measurements becomes more substantial than the GNSS observations, showing that the indirect measurements have more weight in such scenarios. Furthermore, the three lines represent three different integration times (t_i), which signify the duration for which the link is active. It can be seen that as t_i increases, the uncertainty decreases. This is because the same noise gets averaged over a longer period, resulting in a higher Signal-to-Noise Ratio (SNR) and high accuracy range measurements.

The relative uncertainty in the scaling factor f shown in Fig. 2b shows that the density can be estimated within 5% of the nominal value in the best-case scenario. This value, however, is the same as the knowledge of C_D assumed for the simulation. If the knowledge of C_D were exact, the uncertainty in the scaling factor would be the same as the uncertainty in C_D given by Fig. 2a, i.e., with range measurements of cm-level accuracy, the uncertainty of density measurements could be reduced by three orders. Therefore, it can be inferred that the estimation of atmospheric density is limited by the knowledge of the drag coefficient, and high-accuracy range measurements add little value in this use case.

5. CONCLUSIONS

Range measurements performed using laser communication technology can prevent the need for separate instruments on-board the satellites. An application of such a combined system in the estimation of atmospheric

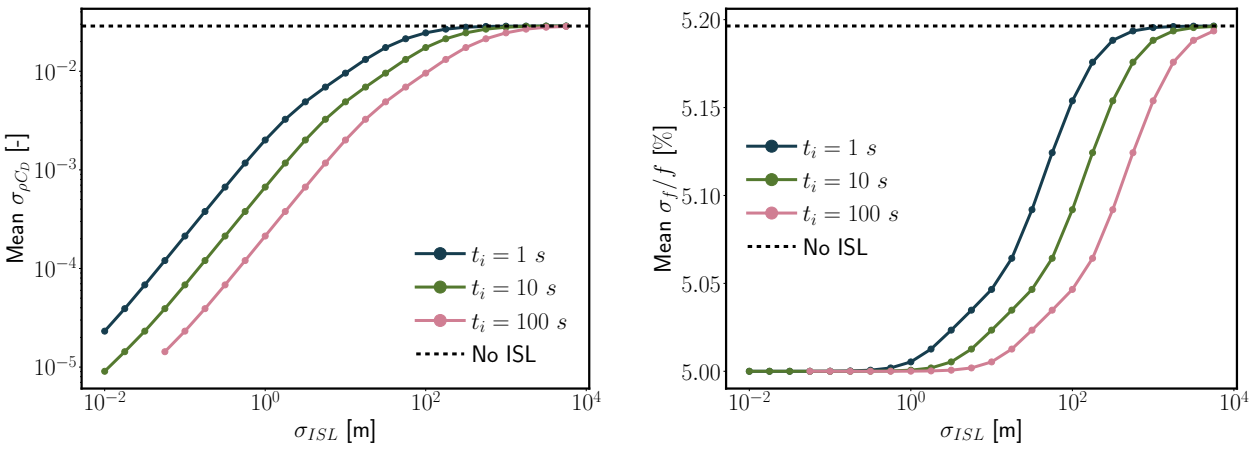

(a) Uncertainty in the drag coefficient.

(b) Relative uncertainty of scaling factor in percentage.

Figure 2: Plot of the standard deviation σ as a function of Inter-Satellite Ranging noise σ_{ISL}, averaged over 24 arcs, for three integration times t_i. The dotted line represents the observation model with only GNSS positions and without ISL range measurements.

density is discussed in this paper. The analysis shows that high-precise direct inter-satellite range measurements using optical communication signals can improve the density estimates compared to GNSS measurements only if the knowledge of the drag coefficient can be improved. Therefore, future work will focus on improving our knowledge of the drag coefficient. Moreover, the actual uncertainty in the optical ISL range measurements will depend on how precisely the transmitted and received communication signals can be time-tagged and correlated. A laser communication system will be modeled and analyzed to compute the achievable ranging performances.

ACKNOWLEDGMENTS

The authors would like to thank the support from the Dutch Research Council (NWO) for funding the Perspective Project P19-13 "Optical Wireless Super Highways." The authors declare that they have no relevant or material financial interests that relate to the research described in this paper.

REFERENCES

[1] Zhang, Z., Deng, L., Feng, J., Chang, L., Li, D., and Qin, Y., "A survey of precision formation relative state measurement technology for distributed spacecraft," *Aerospace* **9**(7), 362 (2022).

[2] Turan, E., Speretta, S., and Gill, E., "Autonomous navigation for deep space small satellites: Scientific and technological advances," *Acta Astronautica* **193**, 56–74 (2022).

[3] Montenbruck, O. and Gill, E., [*Satellite Orbits: Models, Methods and Applications*], Springer, Berlin, Heidelberg (2000).

[4] Kang, Z., Bettadpur, S., Nagel, P., Save, H., Poole, S., and Pie, N., "GRACE-FO precise orbit determination and gravity recovery," *Journal of Geodesy* **94**(9), 85 (2020).

[5] Kaushal, H. and Kaddoum, G., "Optical communication in space: Challenges and mitigation techniques," *IEEE Communications Surveys & Tutorials* **19**(1), 57–96 (2017).

[6] Net, M. S. and Hamkins, J., "Optical telemetry ranging," *The Interplanetary Network Progress Report* **42-221**, 1–23 (2020).

[7] Net, M. S., "Optical ranging: Asynchronous-mode concept, prototype and validation," *The Interplanetary Network Progress Report* **42-232**, 1–18 (2023).

[8] Andrews, K., Hamkins, J., Shambayati, S., and Vilnrotter, V., "Telemetry-based ranging," in [*IEEE Aerospace Conference*], 1–16, IEEE, Big Sky, MT, USA (2010).

[9] Hamkins, J., Kinman, P., Xie, H., Vilnrotter, V., and Dolinar, S., "Telemetry ranging: Concepts," *Interplanetary Network Progress Report* **42-203**, 1–20 (2015).

[10] Hamkins, J., Kinman, P., Xu, Z., Vilnrotter, V., Dolinar, S., Adams, N., Sanchez, E., and Milliard, W., "Telemetry ranging: Laboratory validation tests and end-to-end performance," *IPN Progress Report* **42-206**, 1–35 (2016).

[11] Hamkins, J., Kinmany, P., Xie, H., Vilnrotter, V., and Dolinar, S., "Telemetry ranging: Signal processing," *Interplanetary Network Progress Report* **42-204**, 1–56 (2016).

[12] Vilnrotter, V. and Hamkins, J., "Telecommand telemetry ranging for deep-space applications," in [*IEEE Aerospace Conference*], 1–10, IEEE, Big Sky, MT, USA (2019).

[13] Turan, E., Speretta, S., and Gill, E., "Performance analysis of crosslink radiometric measurement based autonomous orbit determination for cislunar small satellite formations," *Advances in Space Research* **72**(7), 2710–2732 (2023).

[14] Picone, J. M., Hedin, A. E., Drob, D. P., and Aikin, A. C., "Nrlmsise-00 empirical model of the atmosphere: Statistical comparisons and scientific issues," *Journal of Geophysical Research: Space Physics* **107**(A12), SIA 15–1–SIA 15–16 (2002).

[15] Doornbos, E. and H., K., "Modelling of space weather effects on satellite drag," *Advances in Space Research* **37**(6), 1229–1239 (2005).

[16] Dirkx, D., *Interplanetary Laser Ranging*, PhD thesis, Delft University of Technology, The Netherlands (2015).